Tetrahedron: *Asymmetry* xxx (2016) xxx–xxx

Contents lists available at ScienceDirect

Tetrahedron: *Asymmetry*

journal homepage: www.elsevier.com/locate/tetasy

Determination of the absolute configuration of (+)- and (−)-*N*-CBZ-3-fluoropyrrolidine-3-methanol using vibrational circular dichroism and confirmation of stereochemistry by conversion to (*R*)-*tert*-butyl 3-fluoro-3-(((*R*)-1-phenylethyl)carbamoyl)pyrrolidine-1-carboxylate

Panayiotis A. Procopiou [a,*], Richard J. D. Hatley [a], Sean M. Lynn [b], Royston C. B. Copley [b], Yanan He [c], Douglas J. Minick [d]

[a] *Medicinal Chemistry, Fibrosis and Lung Injury DPU, Respiratory Therapeutic Area, GlaxoSmithKline Medicines Research Centre, Gunnels Wood Road, Stevenage SG1 2NY, United Kingdom*
[b] *Platform Technology & Science, GlaxoSmithKline Medicines Research Centre, Gunnels Wood Road, Stevenage, Hertfordshire SG1 2NY, United Kingdom*
[c] *Global Spectroscopy, Structural and Metabolite ID, Platform Technology and Science, GlaxoSmithKline, 709, Swedeland Road, King of Prussia, PA 19087, United States*
[d] *Platform Technology and Science, GlaxoSmithKline, Five Moore Drive, Research Triangle Park, NC 27709-3398, United States*

ARTICLE INFO

Article history:
Received 24 August 2016
Accepted 7 September 2016
Available online xxxx

ABSTRACT

Racemic *N*-CBZ-3-fluoropyrrolidine-3-methanol (±)-**1** was resolved by preparative chiral HPLC. The absolute configuration of the enantiomers of **1** was identified by vibrational circular dichroism and confirmed by chemical synthesis, which involved exchanging the CBZ protecting group of (−)-**1** with Boc, followed by oxidation with $RuCl_3$, $NaIO_4$, activation of the resulting acid with carbonyl diimidazole and reaction with (*R*)-α-methylbenzylamine to give (*R*)-*tert*-butyl 3-fluoro-3-(((*R*)-1-phenylethyl)carbamoyl) pyrrolidine-1-carboxylate **7**. The latter was compared with authentic (*S*)-*tert*-butyl 3-fluoro-3-(((*R*)-1-phenylethyl)carbamoyl)pyrrolidine-1-carboxylate **6** and its diastereomer **7**; the configuration of diastereomer **6** was obtained by an X-ray diffraction study. This established that the enantiomer (−)-**1** had an (*R*)-configuration.

1. Introduction

The introduction of fluorine atoms has many and varied functions in the design and lead optimisation of drug candidates in medicinal chemistry. These include reduction of the pK_a of basic centres, reduction of metabolic clearance and thus improvement of pharmacokinetic properties of compounds, increase in potency, membrane permeability and influencing of compound's conformation. Furthermore, the [^{18}F] isotope is increasingly being used in positron emission tomography (PET) for imaging purposes due to the longer half-life of the [^{18}F] isotope (110 min) compared to [^{11}C] (20 min). Applications of fluorine in medicinal chemistry have recently been reviewed by Gillis et al.[1] Our group was interested in using large quantities of *N*-CBZ-3-fluoropyrrolidine-3-methanol (benzyl 3-fluoro-3-(hydroxymethyl)pyrrolidine-1-carboxylate) **1** as a building block for a medicinal chemistry project focusing on the identification of $\alpha_v\beta_6$ integrin inhibitors[2,3] for their use in the treatment of idiopathic pulmonary fibrosis.[4] A four step synthesis of (±)-**1** has very recently been reported in the patent literature, starting from commercially available *N*-CBZ-3-pyrrolidinone **2** and in 46% overall yield, involving Wittig olefination, fluorobromination, displacement of bromide with potassium acetate and base hydrolysis of the ester group.[5] Racemic **1** was not commercially available at the time this work was initiated, but small quantities are now currently available from two suppliers. The individual enantiomers of **1** are not commercially available, and their synthesis/isolation has so far not been reported in the literature. The lack of publications may reflect the difficulty in introducing enantioselectively the chiral tertiary fluoride moiety, which is also β to a basic centre.

Mykhailiuk et al. described the synthesis of methyl ester **3** using methyl 2-fluoroacrylate and an azomethine ylide by a 1,3-dipolar cycloaddition reaction.[6] The racemic *N*-Boc-3-fluoropyrrolidine-3-methanol **4** is commercially available from a variety of commercial suppliers, but the synthesis/isolation of its enantiomers has not been reported yet.

* Corresponding author. Tel.: +44 1438 790496; fax: +44 1438 768302.
E-mail address: pan.a.procopiou@gsk.com (P.A. Procopiou).

http://dx.doi.org/10.1016/j.tetasy.2016.09.008
0957-4166/

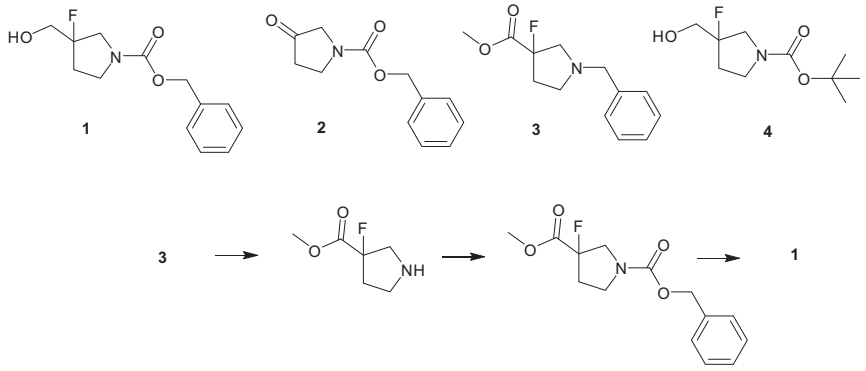

Figure 1. Structures of some 3-fluoropyrrolidines and synthesis of **1** starting from **3**.

Our initial studies used large quantities of racemic **1**, purchased from Wuxi App Tec, who exchanged the benzyl protecting group of **3** with CBZ and then reduced the methyl ester with lithium borohydride (Fig. 1). The resulting racemic alcohol **1** was then resolved by preparative chiral HPLC to give the two enantiomers of **1** as thick colourless oils with high purity and >98:2 enantiomeric ratio.

Whilst the two enantiomers of **1** were fully characterised, their absolute configuration was still not known. Herein, we report the absolute configuration of **1** determined by vibrational circular dichroism (VCD) and the synthesis of a derivative to confirm the stereochemistry.

2. Results and discussion

2.1. Determination of absolute configuration of (−)-1 and (+)-1 by VCD

The absolute configuration of each enantiomer of **1** was determined by comparing the measured VCD and IR spectra of a sample of (−)-**1** with an enantiomeric ratio (e.r.) of 99.5:0.5 (chiral HPLC), and a sample of its enantiomer (+)-**1**, with an e.r. of 99.8:0.2 with the calculated data.

The baseline-corrected VCD and IR spectra of (−)-**1** and (+)-**1** were compared with the calculated spectra, shown in Figures 2 and 3 respectively. The comparison indicated that the VCD spectrum of (+)-**1** is approximately the mirror image of the model spectrum and (−)-**1** coincident with it. With respect to the IR spectra (lower frame in each figure), the spectrum calculated for Model fs1r is in excellent agreement with the experimental IR spectra, supporting (a) the overall structure of these isomers (i.e., their molecular connectivity), and (b) satisfactory coverage of their solution phase conformational space by the computational analysis. These data are consistent with (−)-**1** having the same configuration of the model and (+)-**1** having the opposite configuration as the model. Based on these findings, (−)-**1** was assigned the (*R*)-absolute configuration and (+)-**1** the (*S*)-absolute configuration. The optimised geometry, relative free energy, the Boltzmann and adjusted populations of the calculated conformers of the modelled structure are shown in Figure 4. The confidence level for these assignments was evaluated by Compare*VOA* program (BioTools. Inc., Jupiter, FL).[7] The confidence level of the assignment is >99% based on current database that includes 88 previous correct assignments for different chiral structures (see Section 4).

2.2. Confirmation of the absolute configuration

In addition to the VCD study on the two enantiomers of **1**, we extensively investigated the possibility of identifying the configuration from X-ray diffraction studies. Attempts to crystallise (±)-**1**, (+)-**1**, (−)-**1**, ester derivatives of (+)-**1** and (−)-**1**, salts of the deprotected parent (3-fluoropyrrolidin-3-yl)methanol, amide derivatives of the same or indeed bis-acyl derivatives (ester and amide) all failed to produce suitable crystals.

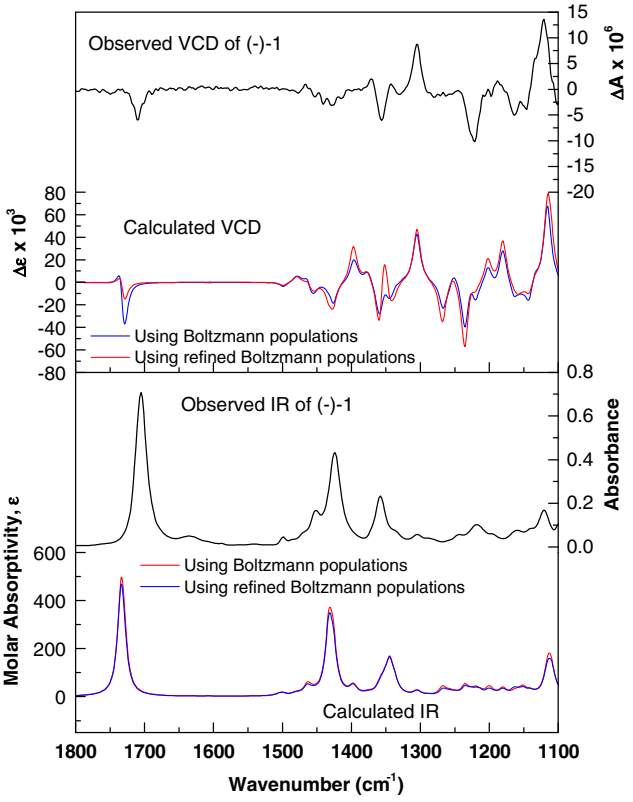

Figure 2. IR (lower frame) and VCD (upper frame) spectra observed for (−)-**1** (right axes) compared with the calculated VCD spectra (left axes) using Boltzmann (red curve) and refined Boltzmann population (blue curve) of the 12 conformations of the modelled R structure of fs1r (left axes).

Having failed with the crystallisation approach, we next investigated a functional group interconversion approach to identify a derivative of **1** whose absolute configuration was unambiguously determined. Mykhailiuk et al. recently reported the conversion of 1-(*tert*-butoxycarbonyl)-3-fluoropyrrolidine-3-carboxylic acid **5** to the two diastereomeric amides **6** and **7**. The structure of **6** was established by X-ray diffraction study to be (*S*)-*tert*-butyl 3-fluoro-3-(((*R*)-1-phenylethyl)carbamoyl)pyrrolidine-1-carboxylate, whereas the configuration of the less polar isomer **7** was inferred as (*R*)-*tert*-butyl 3-fluoro-3-(((*R*)-1-phenylethyl)carbamoyl)pyrrolidine-1-carboxylate (Scheme 1).[8]

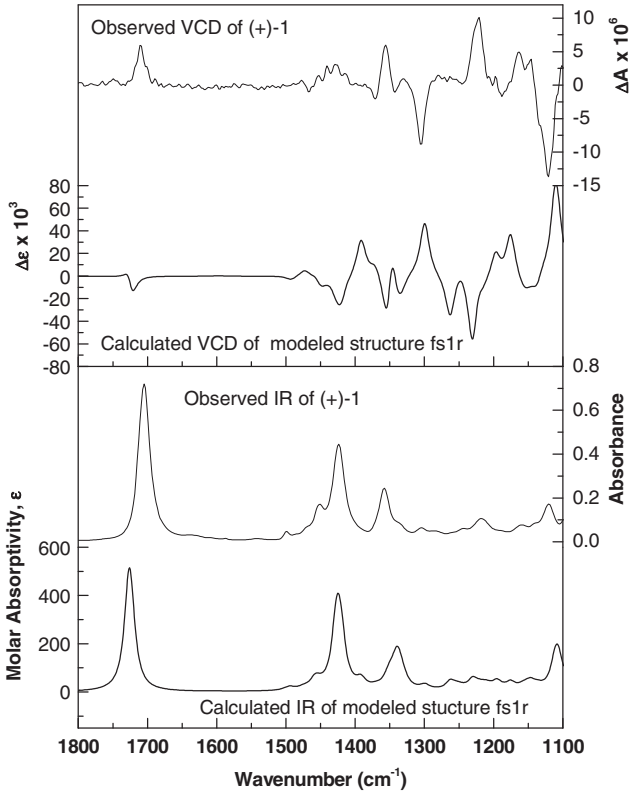

Figure 3. IR (lower frame) and VCD (upper frame) spectra observed for (+)-**1** (right axes) compared with the calculated averaged (refined Boltzmann population) spectra for the 12 conformations of the modelled R structure of fs1r (left axes).

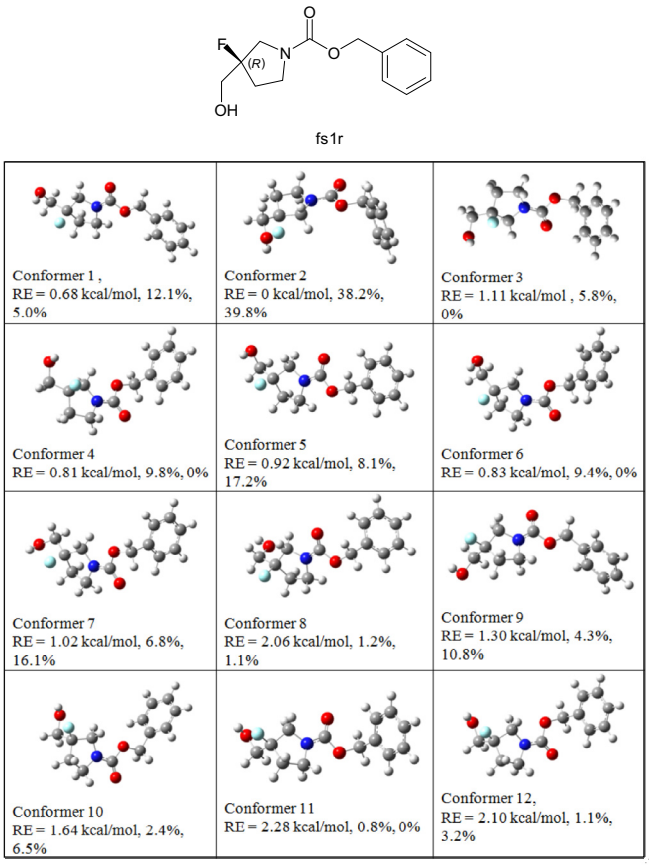

Figure 4. Optimised geometries, relative energies, Boltzmann populations and refined Boltzmann populations of the twelve calculated conformers of the modelled structure of fs1r.

Our investigations started by repeating Mykhailiuk's preparation of amides **6** and **7**. A racemic mixture of commercially available acid **5** was reacted with carbonyl diimidazole (CDI), followed by (+)-(*R*)-α-methylbenzylamine to give a diastereomeric mixture of *N*-α-methylbenzyl amides **6** and **7**. The two diastereomers were separable by normal phase chromatography on silica gel, and the compounds were analysed by LCMS, ^{1}H and ^{13}C NMR spectroscopy, specific rotation and chiral HPLC. The specific rotations for our samples were for **6** $[\alpha]_D^{20} = +73$ (*c* 0.876, MeOH) and for **7** $[\alpha]_D^{20} = +63$ (*c* 0.933, MeOH), whereas the reported values for **6** and **7** are $[\alpha]_D^{20} = +83$ (*c* 0.725, MeOH) and $[\alpha]_D^{20} = +73$ (*c* 0.65, MeOH) respectively. The ^{1}H NMR spectra for the two diastereomers **6** and **7** in $CDCl_3$ were very similar and complicated by the presence of the fluorine atom and rotamers due to the butoxycarbonyl group; however, there were two small diagnostic differences for the pyrrolidine C4-H and the three proton multiplet due to C2-H and C5-H (Scheme 1). We observed the C4-H at 2.22 ppm for the more polar isomer, but it was reported in the literature to be at 2.15 ppm. Furthermore, the multiplet we observed for the less polar isomer at 3.61–3.93 (3H, m) was reported at 3.64–3.92 (3H, m) for the polar isomer. For this reason we generated our own X-ray crystal structure for the more polar diastereomer **6** (Fig. 5). This structure has the same atomic connectivity and absolute structure as that previously published, but is a different solid-state form, with it being anhydrous rather than a monohydrate. Despite our X-ray results for **6** being in broad agreement with the published crystal structure, the reported ^{1}H NMR spectrum differed from the spectrum we obtained.[8] This confirmed that the more polar isomer was indeed **6** and that our spectroscopic data for **6** were correct. After contacting Mykhailiuk et al. they subsequently corrected their originally reported spectroscopic data.[9]

Having unambiguously established the structures of **6** and **7**, we next focussed on converting **1** into either **6** or **7** and comparing the spectroscopic data with those for authentic **6** and **7**. The (−)-enantiomer of **1**, was hydrogenolysed over 10% Pd/C in ethanol to remove the CBZ protecting group, and the resulting amine (−)-**8** was protected with di-*tert*-butyl dicarbonate to give (−)-*tert*-butyl 3-fluoro-3-(hydroxymethyl)pyrrolidine-1-carboxylate **4** (Scheme 2). The latter **4** was oxidised with ruthenium trichloride and sodium periodate in acetonitrile–water overnight and the resulting carboxylic acid **5** was then converted as before into the corresponding amide using CDI and (+)-(*R*)-α-methylbenzylamine. This amide was compared with the authentic amides **6** and **7** and it was found to be identical by NMR spectroscopy, specific rotation and chiral HPLC to (*R*)-*tert*-butyl 3-fluoro-3-(((*R*)-1-phenylethyl)carbamoyl)pyrrolidine-1-carboxylate **7**. Comparative ^{1}H NMR spectroscopic data, chiral HPLC retention times and specific rotations for authentic **6** and **7** and synthetic **7** are summarised in Table 1. Furthermore, overlays of the ^{1}H NMR spectra of these three compounds are shown in Figure 6.

It is noteworthy that the carboxylic acid **5** is unstable under the $RuCl_3$–$NaIO_4$ oxidation conditions. Thus, when alcohol **4** was stirred at room temperature for 5 days in the presence of 0.05 equiv of $RuCl_3$ and 5 equiv of $NaIO_4$ in aqueous acetonitrile, a mixture was observed which contained the expected product **5** [RT = 0.52 min, 14%, ES−ve *m*/*z* 232 $(M-H)^-$] together with an unknown degradation product **9** [RT = 0.45 min, 78%, ES−ve *m*/*z* 226]. This mixture of compounds was difficult to separate, hence the mixture was treated as above with CDI, followed by (*R*)-(+)-α-methylbenzylamine to give a new mixture of amides, which

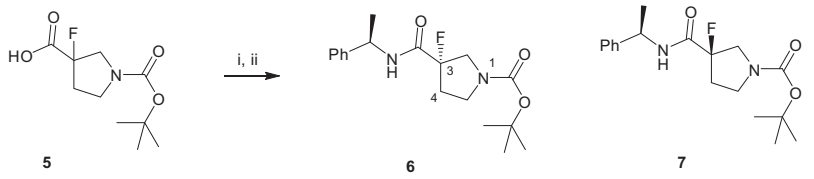

Scheme 1. *Reagents and conditions*: (i) CDI, THF, 80 °C, 1.5 h; (ii) (*R*)-(+)-α-methylbenzylamine, 80 °C, 1.5 h, 28% for **6** and 36% for **7**.

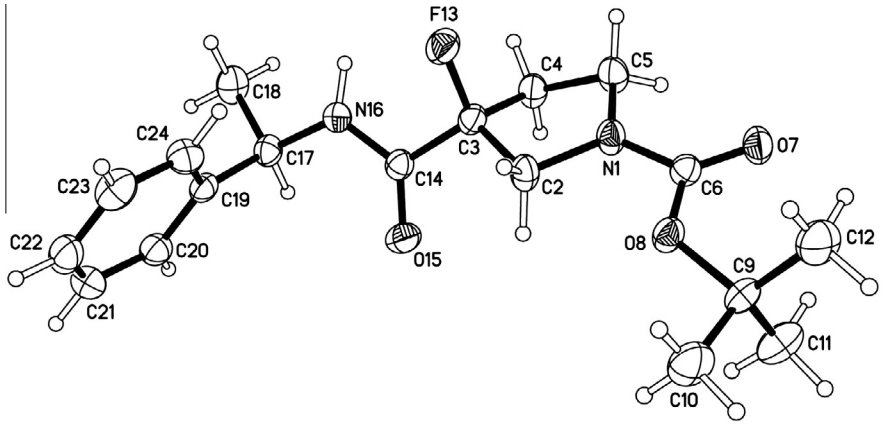

Figure 5. The 2D connectivity and 3D conformation and absolute configuration taken from the crystal structure of **6**. Anisotropic atomic displacement ellipsoids for the non-hydrogen atoms are shown at the 50% probability level. Hydrogen atoms are displayed with an arbitrarily small radius.

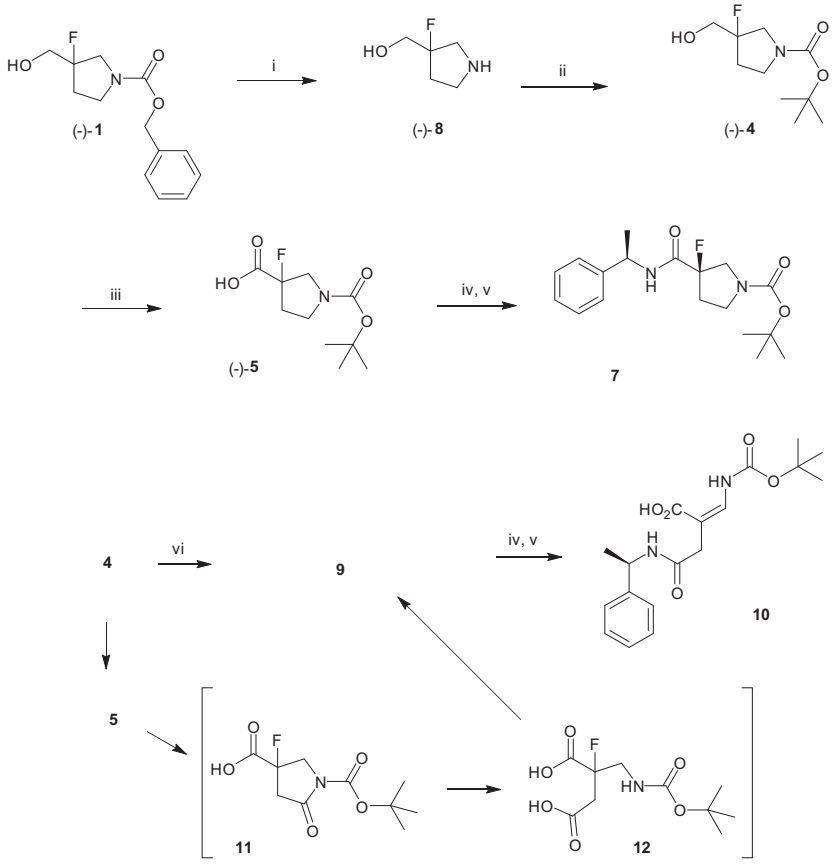

Scheme 2. *Reagents and conditions*: (i) H_2, 10% Pd/C, EtOH, 16 h, 100%; (ii) di-*tert*-butyl dicarbonate, diisopropylethylamine, DCM, 20 °C, 3 h, 79%; (iii) $RuCl_3$, $NaIO_4$, MeCN, water, 20 °C, 16 h, 59%; (iv) CDI, THF, 20 °C, 1 h, 50 °C, 0.5 h; (v) (*R*)-(+)-α-methylbenzylamine, 20 °C, 1.5 h, 5% (for the two steps); (vi) $RuCl_3$, $NaIO_4$, MeCN, water, 20 °C, 5 days, 3%.

Table 1
Comparative data for authentic **6**, **7** and synthetic **7**

Compound	Chiral HPLC[a] RT	$[\alpha]_D^{20}$ in MeOH	^{1}H NMR (500 MHz, $CDCl_3$)
6	9.50 min, 100%	+73 (*c* 0.876)	2.14–2.26 (m, 1H), 3.56–3.87 (m, 3H)
7	7.58 min, 90%	+61 (*c* 1.27)	2.08–2.19 (m, 1H), 3.61–3.93 (m, 3H)
7[b]	7.58 min, 98%	+63 (*c* 1.15)	2.08–2.19 (m, 1H), 3.61–3.93 (m, 3H)

[a] Analytical chiral HPLC was conducted on a Chiralpak AD column (250 mm × 4.6 mm) eluting with 10% EtOH–heptane, flow rate = 1 mL/min, and detecting at 215 nm.
[b] Synthetic sample of **7** derived by the route outlined in Scheme 2.

was purified twice by chromatography on silica, followed by mass-directed auto-preparative HPLC (MDAP). The main component was obtained as an inseparable isomeric mixture LCMS RT = 0.71 min, 20%, ES+ve *m*/*z* 349 $(M+H)^+$ and RT = 0.72 min, 70%, ES+ve *m*/*z* 349 $(M+H)^+$ with the remainder being a multitude of minor components. ^{1}H, ^{13}C NMR, HSQC, HMBC, ^{15}N HMBC, COSY, ROESY spectra were recorded. Spectroscopic examination allowed the elucidation of the structure of the major isomer as amide **10**, to the limits of the data collected and the correlations assigned. The geometry of the double bond was identified as (*Z*) since there was an NOE enhancement between the olefinic hydrogen at 8.03 ppm (br s, 1H) and the allylic methylene at 3.23 and 3.18 ppm each (d, *J* = 14 Hz, 1H). The (*R*)-α-methylbenzylamine was attached to the primary carboxylic acid since there was a correlation between the allylic methylene and the amide nitrogen. The correlations observed for compound **10** in the ^{1}H, ^{13}C and ^{15}N

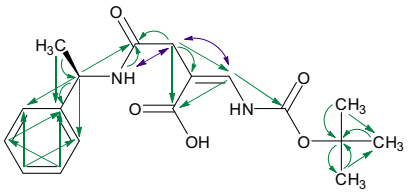

Figure 7. Summary of correlations observed for amide **10**. Key to correlation arrows: green arrows are HMBC correlations and purple arrows are ROESY correlations.

HMBC and ROESY spectra are highlighted in Figure 7. The structure of the minor isomer was not determined, but it might be either the (*E*) geometrical isomer or alternatively the regioisomeric amide. A plausible explanation for the formation of amide **10** from **4** via **5** might be the result of further oxidation of the C5 methylene to give imide **11** (Scheme 2). Efficient oxidation of amides and carbamates to imides, for example *N*-Boc-pyrrolidine to *N*-Boc-butyrolactam in 74% yield, using hypervalent iodine reagents has been reported.[10] Furthermore, oxidation of lactams to cyclic imides using ruthenium tetroxide, generated in situ from catalytic amounts of RuO_2 in the presence of excess $NaIO_4$, is well established.[11–15] Hydrolysis of imide **11** under the prolonged aqueous conditions to give diacid **12**, followed by elimination of hydrogen fluoride from **12** could proceed either from the methylene next to the nitrogen, or next to the carboxylic acid or from both giving rise to a number of products **9**. Finally activation of **9** with CDI and reaction with amine would provide **10**. The (*Z*)-geometry of the double bond however could not be readily deduced.

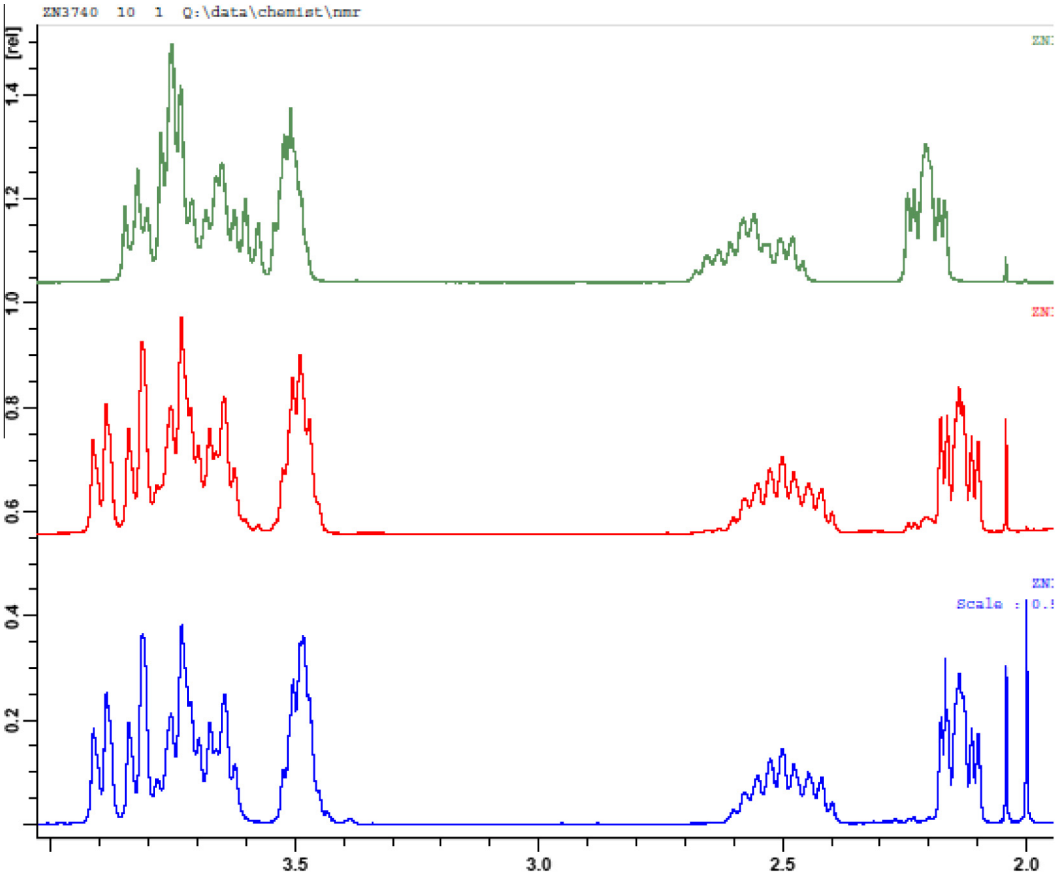

Figure 6. Overlay of ^{1}H NMR spectra of authentic **6** (top spectrum in green), authentic **7** (middle spectrum in red) and synthetic **7** derived by route as shown in Scheme 2 (lower spectrum in blue).

Table 2
Structure, specific rotation and chiral HPLC retention times on Chiralpak AD-H for (+)-**1** and (−)-**1**

Structure	Config.	Compound	$[\alpha]_D^{20}$ in $CHCl_3$	Chiral HPLC[a] RT and % purity
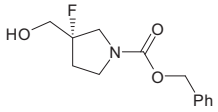	(*S*)	(+)-**1**	+24 (*c* = 0.80)	7.95 min, 99.8%
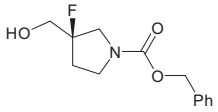	(*R*)	(−)-**1**	−23 (*c* = 1.4)	6.20 min, 99.5%

[a] Analytical chiral HPLC was conducted on a Chiralpak AD-H column (250 mm × 4.6 mm) eluting with 40% EtOH–heptane, flow rate = 1 mL/min, and detecting at 215 nm.

3. Conclusion

Racemic *N*-CBZ-3-fluoropyrrolidine-3-methanol was resolved by preparative chiral HPLC and the absolute configuration of the enantiomers was identified by VCD and confirmed by chemical synthesis. Relevant data for (+)-**1** and (−)-**1** are summarised in Table 2. The (*S*) configuration was assigned to the (+)-**1** enantiomer. An enantioselective synthesis of (+)-**1** will be published in due course.

4. Experimental

4.1. General

TLC was performed on Merck 0.25 mm Kieselgel 60 F_{254} plates. Products were visualised under UV light and/or by staining with aqueous $KMnO_4$ solution. LCMS analysis was conducted on a Waters Acquity UPLC CSH C18 column (2.1 mm × 50 mm i.d. 1.7 μm packing diameter) eluting with 10 mM ammonium bicarbonate in water adjusted to pH 10 with aqueous ammonia (solvent A), and acetonitrile (solvent B), using the following elution gradient: 0.0–1.5 min 3–95% B, 1.5–1.9 min 95% B, 1.9–2.0 min 95–3% B, at a flow rate of 1 mL min^{-1} at 40 °C. The UV detection was an averaged signal from wavelength of 210–350 nm, and mass spectra were recorded on a mass spectrometer using alternate-scan electrospray positive and negative mode ionisation (ES+ve and ES−ve). Column chromatography was performed on disposable, normal phase, SPE cartridges. The accurate mass measurements were performed on a Bruker maXis Impact TOF mass spectrometer, equipped with an ESI interface. ^{1}H NMR spectra were recorded at 400 (Bruker AVII), 500 (Bruker AVI) or 600 MHz (Bruker AVII). The chemical shifts are expressed in ppm relative to tetramethylsilane. ^{13}C chemical shifts of compounds where rotamers were present are given as ranges. Optical rotations were measured with an Optical Activity AA100 digital polarimeter and are given in 10^{-1} deg cm^2 g^{-1}. Analytical chiral HPLC was conducted on Chiralpak AD-H column at room temperature, eluants and conditions are described under individual experiments; detection was performed using UV light at the specified wavelength.

4.2. Resolution of (±)-benzyl 3-fluoro-3-(hydroxymethyl) pyrrolidine-1-carboxylate (±)-1

Resolution of 5 kg of (±)-**1**, dissolved in 40% ethanol-heptane (151.5 g/L) was carried out by preparative chiral HPLC on a Chiralpak AD column (20 cm × 25 cm) operating at 25 °C at a flow rate of 154 L/h with a mobile phase of 20% ethanol in heptane. Injection volume 250 mL, injection mass 38 g/injection, run-time 24 min. Appropriate fractions were combined and evaporated to give:

4.2.1. (−)-Benzyl 3-fluoro-3-(hydroxymethyl)pyrrolidine-1-carboxylate (−)-1

LCMS RT = 0.85 min, 100%, ES+ve *m*/*z* 254 $(M+H)^+$; ^{1}H NMR ($CDCl_3$, 600 MHz) δ 7.40–7.36 (m, 2H), 7.37–7.36 (m, 2H), 7.34–7.30 (m, 1H), 5.19–5.12 (m, 2H), 3.84–3.72 (m, 2H), 3.79–3.68 (m, 1H), 3.77–3.66 (m, 1H), 3.65–3.50 (m, 1H), 3.61–3.50 (m, 1H), 2.23–2.16 (m, 1H), 2.08–1.92 (m, 1H); ^{13}C NMR ($CDCl_3$, 151 MHz) 155.2–154.4 (m, 1C), 137.0–136.3 (m, 1C), 128.5 (s, 2C), 128.1 (s, 1C), 128.0–127.9 (m, 2C), 104.3–101.6 (m, 1C), 67.0 (s, 1C), 65.3–64.7 (m, 1C), 53.9–53.0 (m, 1C), 44.8–44.2 (m, 1C), 33.4–32.2 (m, 1C); ^{19}F NMR ($CDCl_3$, 376.5 MHz) (−159.3)–(−159.6); HRMS (ESI) calcd for $C_{13}H_{17}FNO_3$ 254.1187 $(M+H)^+$, found 254.1190; $[\alpha]_D^{20}$ = −23 (*c* 1.4, $CHCl_3$). Analytical Chiral HPLC RT = 6.48 min, 99.2% on a Chiralpak AD-H column (250 mm × 4.6 mm) eluting with 40% EtOH–heptane, flow-rate = 1.0 mL/min, detecting at 215 nm. A purer analytical sample which was used for the VCD study had Analytical Chiral HPLC RT = 6.20 min, 99.5% on a Chiralpak AD-H column (250 mm × 4.6 mm) eluting with 40% EtOH–heptane, flow-rate = 1.0 mL/min and detecting at 215 nm.

4.2.2. (+)-Benzyl 3-fluoro-3-(hydroxymethyl)pyrrolidine-1-carboxylate (+)-1

LCMS RT = 0.85 min, 98.7%, ES+ve *m*/*z* 254 $(M+H)^+$; ^{1}H NMR ($CDCl_3$, 600 MHz) identical to (−)-**1** spectrum; ^{1}H NMR (600 MHz, DMSO-d_6) δ 7.40–7.35 (m, 4H), 7.33–7.30 (m, 1H), 5.23–5.14 (m, 1H), 5.11–5.04 (m, 2H), 3.66–3.56 (m, 2H), 3.61–3.52 (m, 1H), 3.54–3.42 (m, 2H), 3.47–3.36 (m, 1H), 2.12–1.97 (m, 2H); the spectrum coalesces at high temperature; ^{13}C NMR (151 MHz, DMSO-d_6) δ 153.96–153.76 (m, 1C), 136.99–136.86 (m, 1C), 128.34 (s, 2C), 127.75 (s, 1C), 127.53–127.43 (m, 2C), 104.86–102.22 (m, 1C), 65.88 (s, 1C), 62.83–62.36 (m, 1C), 53.69–52.83 (m, 1C), 44.76–43.95 (m, 1C), 32.65–31.54 (m, 1C); ^{19}F NMR (376.5 MHz, DMSO-d_6) (−155.91)–(−154.81) (m, 1F); HRMS (ESI) calcd for $C_{13}H_{17}FNO_3$ 254.1187 $(M+H)^+$, found 254.1192. $[\alpha]_D^{20}$ = +21 (*c* 2.0, $CHCl_3$); Analytical Chiral HPLC RT = 8.12 min, 97.2% on a Chiralpak AD-H column (250 mm × 4.6 mm) eluting with 40% EtOH–heptane, flow-rate = 1.0 mL/min and detecting at 215 nm. A purer analytical sample which was used for the VCD study had $[\alpha]_D^{20}$ = +24 (*c* 0.80, $CHCl_3$); Analytical Chiral HPLC RT = 7.95 min, 99.8% on a Chiralpak AD-H column (250 mm × 4.6 mm) eluting with 40% EtOH–heptane, flow-rate = 1.0 mL/min and detecting at 215 nm.

4.3. VCD measurements

(−)-**1** and (+)-**1** were dissolved in CD_3CN (11.9 mg/0.2 mL) and placed in a 100 μm pathlength cell with BaF2 windows. IR and VCD spectra were recorded on a Chiral*IR2X*™ VCD spectrometer (BioTools, Inc.) equipped with dual *PEM* accessory, with 4 cm^{-1} resolution, 6-hour collection for both (−)-**1** and (+)-**1**, and

instrument optimised at 1400 cm^{-1}. The IR spectrum of CD_3CN was also measured using the same cell. The baseline of the IR spectra were corrected by subtracting the IR of the solvent from those of the samples, and the baseline corrected VCD spectrum of each sample was obtained by subtracting the VCD of the enantiomer from that of each sample and then divided by two.

4.4. VCD Calculations

A conformational search was carried out using MOE with Amber12:EHT force field and a dielectric constant of 10 for both the molecule and external filed. The conformational search resulted 12 conformers. Geometry optimisation, frequency, and IR and VCD intensity calculations of the conformers resulted from the conformational search were carried out at the DFT level (B3LYP functional/ dgdzvp2 basis set) with Gaussian 09 (Gaussian Inc., Wallingford, CT). The calculated frequencies were scaled by 0.979 and the IR and VCD intensities were converted to Lorentzian bands with 6-cm^{-1} half-width for comparison to experiment. The populations of the conformers were adjusted using the solver function in Excel to obtain the best fit between the experimental and the calculated VCD spectra.

The confidence level in this study was evaluated using CompareVOA™ (BioTools, Inc.), an automated tool for quantifying the level of agreement between calculated and observed VCD data. The confidence level was determined from the absolute values of two parameters from CompareVOA™: total neighbourhood similarity (TNS (VCD)) and the enantiomeric similarity index (ESI).[7] CompareVOA™ results for the current study:

- Analysis range: 1550–1100 cm^{-1}
- Region omitted: Carbonyl stretching
- Range of statistical analysis (minimum 400 cm^{-1}): 450 cm^{-1}
- Width of triangular weighting function: 20 cm^{-1}
- TNS (VCD): 73.1 (absolute value)
- ESI: 70.9 (absolute value)

The confidence level was >99% as the TNS (VCD) value was >70 and ESI >60.

4.5. (*S*)-*tert*-Butyl 3-fluoro-3-(((*R*)-1-phenylethyl)carbamoyl) pyrrolidine-1-carboxylate 6 and (*R*)-*tert*-butyl 3-fluoro-3-(((*R*)-1-phenylethyl)carbamoyl)pyrrolidine-1-carboxylate 7

A solution of (±)-1-(*tert*-butoxycarbonyl)-3-fluoropyrrolidine-3-carboxylic acid **5** (available from Wuxi App Tec) (3.00 g, 12.9 mmol) in THF (70 mL) was treated at room temperature with solid CDI (2.5 g, 15 mmol) and then the mixture was heated to 80 °C for 1.5 h. (*R*)-(+)-α-Methylbenzylamine (1.6 g, 13 mmol) was added at this temperature and then the mixture was heated for a further 1.5 h at 80 °C. The mixture was diluted with ethyl acetate and washed with dilute aqueous HCl, $NaHCO_3$, brine, dried ($MgSO_4$), filtered and allowed to evaporate slowly at room temperature. The mixture was finally concentrated under reduced pressure as no solid crystallised out. The residue was purified by chromatography on two silica cartridges (100 g each) eluting with 0–25% EtOAc–cyclohexane over 40 min. The compound eluting first was obtained as a white foam (1.54 g, 36%): LCMS RT = 1.17 min, ES+ve *m/z* 337 $(M+H)^+$; ^1H NMR (500 MHz, $CDCl_3$) δ 7.39–7.27 (m, 5H), 6.76–6.71 (m, 1H), 5.14 (quin, *J* = 7.1 Hz, 1H), 3.93–3.61 (m, 3H), 3.56–3.43 (m, 1H), 2.62–2.37 (m, 1H), 2.19–2.08 (m, 1H), 1.54 (d, *J* = 7.0 Hz, 3H), 1.49–1.43 (m, 9H), contains about 10% of the more polar diastereomer; ^{13}C NMR ($CDCl_3$,126 MHz) 167.7–167.3 (m, 1C), 154.2–154.0 (m, 1C), 142.5–142.3 (m, 1C), 128.8 (s, 2C), 127.8–127.5 (m, 1C), 126.0 (s, 2C), 103.5–101.0 (m, 1C), 79.9–79.8 (m, 1C), 55.4–54.9 (m, 1C), 49.0 (s, 1C), 44.6–44.2 (m, 1C), 35.7–34.7 (m, 1C), 28.4 (s, 3C), 21.8 (s, 1C); $[\alpha]_D^{20}$ = +61 (*c* 1.27, MeOH); Analytical Chiral HPLC RT = 7.58 min, 90%, and RT = 9.53 min, 10% on a Chiralpak AD column (250 mm × 4.6 mm), eluting with 10% EtOH–heptane, flow rate = 1 mL/min, detecting at 215 nm. A 50 mg portion of this sample was further purified on a silica cartridge (20 g) eluting with 0–25% EtOAc–cyclohexane over 20 min. The appropriate fraction was evaporated under reduced pressure to give an analytically pure sample (30 mg) of (*R*)-*tert*-butyl 3-fluoro-3-(((*R*)-1-phenylethyl)-carbamoyl)pyrrolidine-1-carboxylate (**7**) LCMS RT = 1.16 min, 100%, ES+ve *m/z* 337 $(M+H)^+$ and 354 $(M+NH_4)^+$ and ES−ve *m/z* 335 $(M-H)^-$; $[\alpha]_D^{20}$ = +63 (*c* 0.933, MeOH).

The second compound eluting from the first column (more polar diastereomer) (1.2 g, 28%) was crystallised from diethyl ether to give white crystals of (*S*)-*tert*-butyl 3-fluoro-3-(((*R*)-1-phenylethyl)carbamoyl)pyrrolidine-1-carboxylate **6**: mp = 113–115 °C (diethyl ether); LCMS RT = 1.16 min, 100%, ES+ve *m/z* 337 $(M+H)^+$; ^1H NMR (500 MHz, $CDCl_3$) δ 7.40–7.27 (m, 5H), 6.73 (br s, 1H), 5.14 (quin, *J* = 7.1 Hz, 1H), 3.87–3.56 (m, 3H), 3.55–3.46 (m, 1H), 2.70–2.44 (m, 1H), 2.26–2.14 (m, 1H), 1.54 (d, *J* = 7.0 Hz, 3H), 1.48–1.43 (m, 9H); ^{13}C NMR ($CDCl_3$,126 MHz) 167.7–167.4 (m, 1C), 154.1–154.0 (m, 1C), 142.3–142.2 (m, 1C), 128.8 (s, 2C), 127.7 (s, 2C), 126.1–125.9 (m, 1C), 103.5–101.0 (m, 1C), 80.0–79.7 (m, 1C), 55.4–54.9 (m, 1C), 49.1–48.9 (m, 1C), 44.6–44.2 (m, 1C), 35.5–34.8 (m, 1C), 28.4 (s, 3C), 21.9–21.7 (m, 1C); $[\alpha]_D^{20}$ = +73 (*c* 0.876, MeOH); Analytical Chiral HPLC RT = 9.50 min, 100% on a Chiralpak AD column (250 mm × 4.6 mm) eluting with 10% EtOH–heptane, flow rate = 1 mL/min, detecting at 215 nm. The absolute configuration of this diastereomer was established from an X-ray diffraction study.

4.6. Crystal data and refinement for 6

$C_{18}H_{25}FN_2O_3$; *M* = 336.40; colourless hexagonal prism; 0.20 × 0.14 × 0.14 mm; *T* = 150(2) K; orthorhombic; space group, $P2_12_12_1$ (no. 19); unit cell dimensions, *a* = 6.08015(9) Å, *b* = 12.26945(19) Å, *c* = 24.2480(4) Å, *V* = 1808.90(5) $Å^3$; *Z* = 4; d_{calc} = 1.235 Mg m^{-3}; μ(Cu-K_α, λ = 1.54178 Å) = 0.750 mm^{-1}; 11153 measured reflections (between 3.65° and 72.30° in θ) of which 3358 unique (R_{int} = 0.0332); R_1 [$I > 2\sigma(I)$] = 0.0275; wR_2 (all data) = 0.0756; absolute structure parameter = −0.02(11).

Crystallographic data for the structure of **6** have been deposited with the Cambridge Crystallographic Data Centre as supplementary publication no. CCDC-1487805. Copies of the data can be obtained, free of charge, on application to CCDC, 12 Union Road, Cambridge CB2 1EZ, UK, (fax: +44-(0)1223-336033 or e-mail: deposit@ccdc.cam.ac.uk).

4.7. (−)-(*R*)-(3-Fluoropyrrolidin-3-yl)methanol 8

A solution of (−)-*N*-CBZ-3-fluoro-3-(hydroxymethyl)pyrrolidine, (−)-**1** (4.0 g, 16 mmol) was hydrogenated over 10% Pd/C (400 mg) in ethanol (150 mL) overnight. The catalyst was removed by filtration through Celite and washed with ethanol. The filtrate and washings were evaporated under reduced pressure to give a yellow oil, which solidified into a waxy solid. The solid (2.0 g) contained some ethanol by NMR and was further dried in a blow-down unit under nitrogen at 40 °C to give **8** in quantitative yield: LCMS RT = 0.22 min, ES+ve *m/z* 120 $(M+H)^+$ and ES−ve *m/z* 118 $(M-H)^-$; $[\alpha]_D^{20}$ = −4 (*c* 1.19, EtOH); ^1H NMR (500 MHz, $CDCl_3$) δ 3.82 (dd, *J* = 18.7, 12.5 Hz, 1H), 3.73 (dd, *J* = 22.0, 12.2 Hz, 1H), 3.22–3.15 (m, 1H), 3.23–3.14 (m, 1H), 2.99–2.92 (m, 1H), 2.91 (dd, *J* = 29.1, 13.2 Hz, 1H), 2.66 (br s, 2H), 2.10–1.98 (m, 1H), 1.94–1.81 (m, 1H); ^{13}C NMR ($CDCl_3$,126 MHz) 106.2 (d, *J* = 175.9 Hz, 1C), 65.6 (d, *J* = 26.6 Hz, 1C), 55.2 (d, *J* = 25.9 Hz, 1C), 46.1 (s, 1C), 35.4 (d, *J* = 22.7 Hz, 1C).

4.8. (−)-(*R*)-*tert*-Butyl 3-fluoro-3-(hydroxymethyl)pyrrolidine-1-carboxylate 4

A solution of (*R*)-(3-fluoropyrrolidin-3-yl)methanol **8** (1.88 g, 15.8 mmol) in DCM (15 mL) and diisopropylethylamine (4.13 mL, 23.7 mmol) was treated with di-*tert*-butyl dicarbonate (3.79 g, 17 mmol) and the mixture was stirred at 20 °C for 3 h. The mixture was partitioned between 2 M HCl and DCM and separated in a phase separator cartridge. The organic layer was concentrated under reduced pressure and the residue was purified by chromatography on a silica cartridge (70 g) eluting with a gradient of 0–50% EtOAc–cyclohexane over 40 min. The fractions were checked by TLC on silica (50% EtOAc–cyclohexane) and stained with $KMnO_4$ solution. Appropriate fractions were combined and evaporated under reduced pressure to give **4** (2.73 g, 79%) as a colourless oil: LCMS RT = 0.79 min, ES+ve *m*/*z* 220 $(M+H)^+$ and 439 $(2M+H)^+$; $[\alpha]_D^{20} = -28$ (*c* 3.51, $CHCl_3$); ^1H NMR (400 MHz, DMSO-d_6) δ 4.90 (t, *J* = 5.8 Hz, 1H), 3.69–3.62 (m, 1H), 3.61–3.54 (m, 1H), 3.50–3.42 (m, 2H), 3.41–3.32 (m, 2H), 2.14–1.96 (m, 2H), 1.42 (s, 9H); ^{13}C NMR (101 MHz, DMSO-d_6) δ 153.2, 103.8, 102.0, 78.1, 62.6, 62.3, 52.9, 52.6, 43.8, 40.1, 32.0, 31.8, 27.8.

4.9. (*R*)-*tert*-Butyl 3-fluoro-3-(((*R*)-1-phenylethyl)carbamoyl) pyrrolidine-1-carboxylate 7

A solution of (−)-*tert*-butyl 3-fluoro-3-(hydroxymethyl)pyrrolidine-1-carboxylate **4** (200 mg, 0.9 mmol) in MeCN (1 mL) and water (1 mL) was treated with $RuCl_3$ (9.5 mg, 0.05 mmol) and sodium periodate (976 mg, 4.5 mmol) and the mixture was stirred at 20 °C for 16 h. The mixture was acidified with 1 M HCl (5 mL) and partitioned in DCM. The aqueous phase was re-extracted twice with DCM and the phases separated in a phase-separation cartridge. The organic solution was evaporated in a blow-down unit to give (*R*)-1-(*tert*-butoxycarbonyl)-3-fluoropyrrolidine-3-carboxylic acid **5** (125 mg, 59%): MS ES−ve *m*/*z* 232 $(M-H)^-$. The acid (125 mg, 0.54 mmol) was dissolved in ethyl acetate (10 mL) and treated with CDI (360 mg, 2.2 mmol) and the mixture was stirred at room temperature for 1 h and then heated at 50 °C for 0.5 h. The mixture was concentrated in a blow-down unit, the residue was dissolved in THF (6 mL) and treated with (*R*)-(+)-α-methylbenzylamine (200 mg, 1.9 mmol) and stirred at 20 °C for 1.5 h. The mixture was diluted with ethyl acetate and washed with 2 M HCl solution twice, followed by brine. The organic solution was dried ($MgSO_4$) and evaporated under reduced pressure to give a grey solid (290 mg). The residue was dissolved in MeOH-DMSO (1:1; 3 mL) and purified by MDAP on a XSELECT CSH C18 column (150 mm × 30 mm i.d. 5 µm packing diameter) at ambient temperature, eluting with a gradient of 30–85% (10 mM ammonium bicarbonate in water adjusted to pH 10 with aq ammonia solution–acetonitrile) running for 30 min, detecting at 254 nm and collecting the peak with RT = 17.4 min, ES+ve *m*/*z* 337 $(M+H)^+$. The fraction was concentrated in a blow-down unit at 45 °C under nitrogen and the residual suspension was extracted with EtOAc. The organic solution was washed with 2 M HCl twice and then with brine, dried ($MgSO_4$) and evaporated under reduced pressure to give a yellow gum (35 mg). The gum was re-purified by MDAP on a XBridge C18 column (100 mm × 19 mm i.d. 5 µm packing diameter) at ambient temperature eluting with a gradient of (10 mM ammonium bicarbonate in water adjusted to pH 10 with aq ammonia solution–acetonitrile) running for 25 min, detecting at 254 nm) collecting the first fraction (RT = 10 min). The solvent was removed in a blow-down unit under nitrogen at 45 °C to give **7** (16 mg, 5%) as a colourless gum: LCMS RT = 1.16 min, ES+ve *m*/*z* 337 $(M+H)^+$, 354 $(M+NH_4)^+$; Analytical Chiral HPLC RT = 7.58 min, 97.7% on a Chiralpak AD column (250 mm × 4.6 mm) eluting with 10% EtOH–heptane, flow rate = 1 mL/min, detecting at 215 nm; $[\alpha]_D^{20} = +63$ (*c* 1.15, MeOH). The ^1H NMR spectrum (500 MHz, $CDCl_3$) as well as the optical rotation and the chiral HPLC RT all match those of authentic (*R*)-*tert*-butyl 3-fluoro-3-(((*R*)-1-phenylethyl)carbamoyl)pyrrolidine-1-carboxylate **7** (Table 1 and Fig. 6).

4.10. (*R*,*Z*)-2-(((*tert*-Butoxycarbonyl)amino)methylene)-4-oxo-4-((1-phenylethyl)amino)butanoic acid 10

A solution of **4** (440 mg, 2.0 mmol) in MeCN (6 mL) and water (6 mL) was treated with $RuCl_3$ (21 mg, 0.1 mmol) and sodium periodate (2.15 g, 10 mmol) and the mixture was stirred at 20 °C for 5 days. The mixture was acidified with 1 M HCl (8 mL) and partitioned in DCM. The aqueous phase was re-extracted twice with DCM and the phases were separated in a phase-separation cartridge. The organic solution was evaporated under reduced pressure and the residue was applied to an aminopropyl cartridge (10 g), washed with DCM (2CV), EtOH (1CV) and MeOH (1CV), and then eluted with 2 M ammonia in MeOH (4CV). The ammoniacal fractions were concentrated under reduced pressure to give a pale yellow solid (460 mg) which was a mixture by LCMS RT = 0.52 min, 13%, ES−ve *m*/*z* 232 $(M-H)^-$ (for the carboxylic acid **5**) and RT = 0.45 min, 78%, ES−ve *m*/*z* 226 and a weak ion at 243). The crude mixture (460 mg) was dissolved in THF (10 mL), treated at 20 °C with solid CDI (352 mg, 2.17 mmol) and then the mixture was heated to 80 °C for 1.5 h. (*R*)-(+)-α-methylbenzylamine (239 mg, 1.97 mmol) was added at this temperature and then the mixture was heated for 1.5 h at 80 °C. The mixture was diluted with ethyl acetate and washed with dilute HCl, aqueous $NaHCO_3$, brine, dried ($MgSO_4$), filtered and concentrated under reduced pressure. The residue was purified by chromatography on silica (50 g) eluting with 0–50% EtOAc–cyclohexane and then further purified on another silica cartridge (20 g) eluting with 0–25% EtOAc–cyclohexane. The appropriate fractions were combined and evaporated under reduced pressure. The residue was however still impure, so it was further purified by MDAP on a Xbridge C18 column (100 mm × 30 mm i.d. 5 µm packing diameter) at ambient temperature, eluting with a gradient of 10 mM ammonium bicarbonate in water adjusted to pH 10 with aqueous ammonia solution in acetonitrile, flow-rate 40 mL/min and detecting between 210 and 350 nm. The appropriate fractions having a mass ion of 349 were concentrated under reduced pressure to give **10** (23 mg, 3%) as a colourless gum: LCMS RT = 0.71 min, 20% and RT = 0.72 min, 70%, ES+ve *m*/*z* 349 $(M+H)^+$; ^1H NMR ($CDCl_3$, 600 MHz) 8.80 (br s, 1H), 8.03 (br s, 1H), 7.32–7.28 (m, 2H), 7.28–7.25 (m, 2H), 7.25–7.21 (m, 1H), 6.88 (br, d, *J* = 7.3 Hz, 1H), 5.02 (quin, *J* = 7.2 Hz, 1H), 3.23 (d, *J* = 14.0 Hz, 1H), 3.18 (d, *J* = 14.0 Hz, 1H), 1.49 (s, 9H), 1.45 (d, *J* = 7.0 Hz, 3H); ^{13}C NMR ($CDCl_3$, 151 MHz): 172.5 (s, 1C), 170.7 (s, 1C), 152.3 (br s, 1C), 143.0 (s, 1C), 139.5 (br s, 1C), 128.6 (s, 2C), 127.2 (s, 1C), 125.9 (s, 2C), 103.2 (br s, 1C), 82.1 (br s, 1C), 49.1 (s, 1C), 33.8 (br s, 1C), 28.1 (s, 3C), 21.9 (s, 1C).

Acknowledgements

The authors are all employees of GSK. We thank Professor William Clegg and Dr. Michael R. Probert from Newcastle University for the GSK funded X-ray crystal structure, Dr. Bill J. Leavens for collecting the HRMS data, Mr. Eric Hortense for the analytical chiral HPLC, Dr. Richard Upton for the 600 MHz NMR spectrum of (+)-**1** in DMSO-d_6, David Thornton, Xiqin Yang and Leo Hsu for the large scale resolution of **1**, and Mr. Samuel Sackville for the attempted crystallisations of (+)-**1**, (−)-**1**, and various derivatives and salts of **8**.

A. Supplementary data

Supplementary data associated with this article can be found, in the online version, at http://dx.doi.org/10.1016/j.tetasy.2016.09.008.

References

1. Gillis, E. P.; Eastman, K. J.; Hill, M. D.; Donnelly, D. J.; Meanwell, N. A. *J. Med. Chem.* **2015**, *58*, 8315–8359.
2. Anderson, N. A.; Campbell-Crawford, M. H. J.; Hancock, A. P.; Pritchard, J. M.; Redmond, J. M. Patent WO2016046225 (31 Mar 2016).
3. Anderson, N. A.; Campbell-Crawford, M. H. J.; Hancock, A. P.; Pritchard, J. M.; Redmond, J. M. Patent WO2016046226 (31 Mar 2016).
4. Nanthakumar, C. B.; Hatley, R. J. D.; Lemma, S.; Gauldie, J.; Marshall, R. P.; Macdonald, S. J. F. *Nat. Rev. Drug Disc.* **2015**, *14*, 693–720.
5. Chen, K. X.; Dong, L.; Estrada, A.; Gibbons, P.; Huestis, M.; Kellar, T.; Liu, W.; Lyssikatos, J. P.; Ma, C.; Olivero, A,; Patel, S.; Shore, D.; Siu, M. Patent WO2014177060 (6 Nov 2014).
6. Yarmolchuk, V. S.; Mykhailiuk, P. K.; Komarov, I. V. *Tetrahedron Lett.* **2011**, *52*, 1300–1302.
7. Debie, E.; De Gussem, E.; Dukor, R. K.; Herrebout, W.; Nafie, L. A.; Bultinck, P. *ChemPhysChem* **2011**, *12*, 1542–1549.
8. Yarmolchuk, V. S.; Mykhalchuk, V. L.; Mykhailiuk, P. K. *Tetrahedron* **2014**, *70*, 3011–3017.
9. Yarmolchuk, V. S.; Mykhalchuk, V. L.; Mykhailiuk, P. K. *Tetrahedron* **2015**, *71*, 7083–7084.
10. Ochiai, M.; Kajishima, D.; Sueda, T. *Tetrahedron Lett.* **1999**, *40*, 5541–5544.
11. Berkowitz, L. M.; Rylander, P. N. *J. Am. Chem. Soc.* **1958**, *80*, 6682–6684.
12. Sheehan, J. C.; Tulis, R. W. *J. Org. Chem.* **1974**, *39*, 2264–2267.
13. Bettoni, G.; Carbonara, G.; Franchini, C.; Tortorella, V. *Tetrahedron* **1981**, *37*, 4159–4164.
14. Sperry, J. *Synthesis* **2011**, 3569–3580.
15. Amat, M.; Pinto, A.; Griera, R.; Bosch, J. *Chem. Eur. J.* **2015**, *21*, 12804–12808.